Reaction Kinetics of Freeze-Granulated NiO/MgAl 2 O 4 Oxygen Carrier Particles for Chemical-Looping Combustion

4 AUTHORS, INCLUDING:

Borje S Gevert
Ecotraffic

31 PUBLICATIONS   **936** CITATIONS

SEE PROFILE

Reaction Kinetics of Freeze-Granulated NiO/MgAl₂O₄ Oxygen Carrier Particles for Chemical-Looping Combustion

Qamar Zafar,*,† Alberto Abad,‡ Tobias Mattisson,§ and Börje Gevert†

Applied Surface Chemistry, Department of Chemical and Biological Engineering, Chalmers University of Technology, S-412 96 Göteborg, Sweden, Instituto de Carboquímica (CSIC), Department of Energy and Environment, Miguel Luesma Castán 4, E-50018 Zaragoza, Spain, and Department of Energy and Environment, Chalmers University of Technology, S-412 96 Göteborg, Sweden

The kinetics of reduction and oxidation of Ni based oxygen carrier particles with CH_4 and O_2 have been investigated. The kinetic parameters were obtained from reactivity data using a thermogravimetric analyzer (TGA), where the freeze-granulated particles were tested using different reactant gas concentrations, temperatures, and particles sizes. The particles showed high reactivity during both reduction and oxidation at temperatures above 900 °C. The shrinking-core model for spherical grain geometry of the reacting particle with chemical reaction control was used to determine the kinetic parameters during both the reduction and oxidation reactions. The reaction order found was 0.4 and 1 for CH_4 and O_2, respectively, while the activation energies found were 114 and 40 kJ/mol for reduction and oxidation reactions, respectively. The reactivity data and kinetic parameters were used to estimate the solid inventory needed in a chemical-looping combustion (CLC) system. The total solid inventory varies with the solid conversion at the inlet of the fuel and air reactor, and for the investigated particles, the minimum solid inventory was 22 kg/MW$_f$. It was found that to operate fuel and air reactors of a CLC system at 950 and 1000 °C, respectively, using an NiO/MgAl₂O₄ oxygen carrier with a 50% active NiO content, the conversion variation between the two reactors should not exceed 0.18. The recirculation rate between the air and fuel reactors needed was 4.15 kg/(s MW$_f$). The high reactivity of the NiO/MgAl₂O₄ both with methane and oxygen found in this work, together with the good fluidizing properties found in earlier studies, suggests that this is an excellent oxygen carrier for a CLC system.

1. Introduction

Combustion of fossil fuels for power generation emits a significant amount of greenhouse gas CO_2 to the atmosphere. It is generally accepted that reduction in greenhouse gas emission is necessary to avoid major climate changes. Chemical-looping combustion (CLC) has emerged as a new combustion technology in which gaseous fuel is burned and resulting CO_2 is inherently separated from the rest of the flue gases.[1−3] The CLC system is composed of two fluidized bed reactors, an air reactor and a fuel reactor; see Figure 1. In CLC, fuel and air never mix; instead, a metal oxide is used as an oxygen carrier which transfers oxygen from air to the fuel reactor. Fuel is oxidized by the metal oxide in the fuel reactor according to

$$(2n + m)M_yO_x + C_nH_{2m} \Longrightarrow (2n + m)M_yO_{x-1} + nCO_2 + mH_2O \quad (1)$$
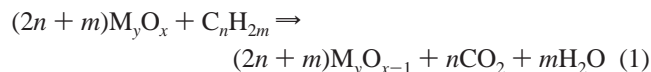
where M_yO_x is a fully oxidized oxygen carrier and M_yO_{x-1} is the oxygen carrier in reduced form.

Figure 1. Chemical-looping combustion.

The exit stream from the fuel reactor contains only CO_2 and H_2O. Thus, pure CO_2 can be obtained by condensing H_2O. The reduced metal oxide, M_yO_{x-1}, is sent to the air reactor, where it is oxidized according to

$$M_yO_{x-1} + \tfrac{1}{2}O_2 \Longrightarrow M_yO_x \quad (2)$$

The flue gas stream from the air reactor will contain N_2 and some unreacted O_2. The reaction between fuel and metal oxide in the fuel reactor may be endothermic as well as exothermic depending on the oxygen carrier used, while the reaction in the air reactor is always exothermic. Since air and fuel never mix in CLC and combustion takes place without flame at a temperature below 1400 °C, NO_x formation should be avoided.[4,5]

* To whom correspondence should be addressed. Telephone: +46-31-7722964. Fax: +46-31-160062. E-mail: zafar@chem.chalmers.se.
† Department of Chemical and Biological Engineering, Chalmers University of Technology.
‡ Instituto de Carboquímica (CSIC), Department of Energy and Environment.
§ Department of Energy and Environment, Chalmers University of Technology.

(1) Richter, H. J.; Knoche, K. F.; Reversibility of combustion processes *ACS Symp. Ser.* **1983**, 71−85.
(2) Ishida, M.; Zheng, D.; Akehata, T. *Energy* **1987**, *12*, 147−154.
(3) Lyngfelt, A.; Leckner, B.; Mattisson, T. *Chem. Eng. Sci.* **2001**, *56*, 3101−3113.
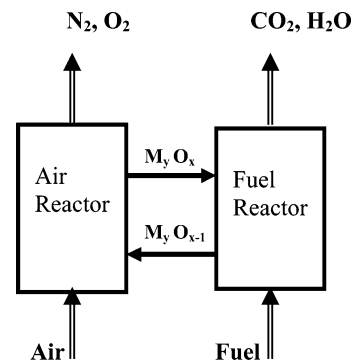(4) Ishida, M.; Jin, H. *Ind. Eng. Chem. Res.* **1996**, *35*, 2469−2472.

The technology has been successfully demonstrated in 10 and 50 kW prototypes of interconnected fluidized beds.[5−7]

Oxygen carriers based on transition state metals Mn, Fe, Co, Ni, and Cu supported on different inert material, e.g., SiO_2, TiO_2, Al_2O_3, MgO, YSZ, and $MgAl_2O_4$, have been investigated for chemical-looping combustion. In general, NiO exhibits very high reactivity and has been successfully used as an oxygen carrier in prototypes based on interconnected fluidized beds of 10 and 50 kW, respectively.[5,6] A number of research groups have tested different types of oxygen carriers with different types of inert materials. A detailed review of this work can be found in Mattisson et al.[8]

Of the investigated oxygen carriers, the system of NiO and $MgAl_2O_4$ seems to be very promising. Zafar et al. investigated oxides of Ni, Mn, Fe, and Cu supported on $MgAl_2O_4$ prepared by impregnation in a TGA using 10% CH_4 for reduction and 5% O_2 for oxidation and concluded that $NiO/MgAl_2O_4$ is a promising candidate both for CLC and CLR (chemical-looping reforming) due to its high reactivity during reduction and excellent regenerability.[9] Villa et al. investigated $NiO/NiAl_2O_4$ and $NiO/MgAl_2O_4$ carriers using CH_4 as fuel. It was concluded that the presence of $NiAl_2O_4$ spinel in the oxygen carrier prevents the crystal size growth of NiO and that Mg addition in the particles limits the sintering of the cubic oxide phase and improves regenerability upon repeated redox cycles.[10] Mattisson et al. investigated NiO supported on $NiAl_2O_4$, $MgAl_2O_4$, TiO_2, and ZrO_2 in a laboratory fluidized bed reactor.[11] All oxygen carriers showed high reactivity, and no particle breakage or agglomeration was observed. $NiO/MgAl_2O_4$ prepared by freeze-granulation has also been successfully used in a 300 W continuous reactor both for chemical-looping combustion (CLC) and chemical-looping reforming (CLR) and has shown excellent results.[12,13] The operation time for CLC was 30 h, and for CLR was 41 h using syngas and natural gas as fuels in the experiments.

Some research has been performed to determine the kinetics of the reaction between oxygen carriers and the common gases used for CLC, and a review of this work follows below.

Ishida et al. studied the kinetics of NiO/YSZ particles prepared by the dissolution method and used the unreacted shrinking-core model to interpret the experimental results. It was concluded that the reduction reaction with hydrogen is controlled by chemical reaction resistance while oxidation is the intermediate reaction between the chemical reaction and ash-layer diffusion. The activation energy was 82 kJ/mol for the reduction reaction and between 17 and 56 kJ/mol for the reaction with air.[14] Ryu et al. studied kinetics of NiO/bentonite and used the unreacted shrinking-core model to interpret the reduction and oxidation reactions. Here, the fuel gas was methane and the oxidizing gas was oxygen. It was concluded that the reduction reaction was controlled by chemical reaction while the oxidation reaction was controlled by product-layer diffusion.[15] The activation energies for the reduction and oxidation reactions were about 9 and 31 kJ/mol, respectively. Garcia-Labiano and co-workers determined the kinetics of reduction with CH_4, CO, and H_2 and of oxidation with O_2 for oxygen carriers based on Ni, Fe, and Cu. They used the shrinking-core model for the platelike geometry for the Cu-based oxygen carrier prepared by impregnation and for the spherical grains geometry for the freeze-granulated Ni- and Fe-based oxygen carriers for the interpretation of the results. It was concluded that both reduction and oxidation reactions are controlled by chemical reaction resistance.[16−18] Only in the case of NiO reduction with H_2 was diffusion resistance included in the model.[17] The value of the activation energy for the reduction reaction was dependent on the fuel gas used and varied between 14 and 78 kJ/mol, and the activation energy for the oxidation reaction was between 7 and 15 kJ/mol. The reaction order found was in the range of 0.25 and 1, depending on the reaction gas and oxygen carrier. Son and Kim investigated the kinetics of $NiO-Fe_2O_3$/bentonite particles using methane as fuel and found that the modified volumetric model is the best representation of the reduction reaction, while the shrinking-core model is the best representation of the oxidation reaction.[19] The values of the activation energy found were in the range of 30−60 and 2−6 kJ/mol for the reduction and oxidation reactions, respectively, depending on the NiO/Fe_2O_3 ratio in the particles. Readman et al. investigated the kinetics of $NiO/NiAl_2O_4$ and found two-step reduction behavior.[20] The first reduction reaction is very fast where oxygen transport to the particle surface is not rate limiting followed by slower reduction where oxygen transport through the particle becomes a rate-limiting step. The reaction order with respect to H_2 and O_2 found was 1, whereas the reaction order with respect to CH_4 was a little bit less than 1.

The reaction kinetics of oxygen carrier particles is a key in designing the air and fuel reactors of a CLC system. Thus, the purpose of this paper is to determine the kinetics of reduction with methane and oxidation with O_2 of an $NiO/MgAl_2O_4$ oxygen carrier prepared by freeze-granulation. In a real system, the fuel would likely be natural gas, but as methane is the main component of natural gas, it will be used in this study for simplicity. To establish the kinetic parameters, the reactions were carried out at different temperatures, gas concentrations, and particles sizes. Further, the kinetic parameters obtained were used to estimate the solid inventory needed in a CLC system.

2. Experimental Details

2.1. Oxygen Carrier Particles. Oxygen carrier particles used in this work were composed of 60 wt % NiO and 40 wt % $MgAl_2O_4$ and were prepared by freeze-granulation. The particles were sintered

(5) Ryu, H. J.; Jin, G.-T.; Yi, C.-K. Demonstration of inherent CO_2 separation and no NOx emission in a 50kW Chemical-looping combustor: Continuous Reduction and Oxidation experiments. Presented at the 7th International Conference on Greenhouse Gas Control Technologies, Vancouver, Canada, Sept 5−9, 2004.

(6) Lyngfelt, A.; Kronberger, B.; Adanez, J.; Morin, J. X.; Hurst, P. The GRACE project. Development of oxygen carrier particles for chemical-looping combustion. Design and operation of a 10 kW chemical-looping combustor. Presented at the 7th International Conference on Greenhouse Gas Control Technologies, Vancouver, Canada, Sept 5−9, 2004.

(7) Adanez, J.; Gayan, P.; Celaya, J.; de diego, L.; Garcia-Labiano, F.; Abad, A. *Ind. Eng. Chem. Res.* **2006**, *45*, 6075−6080.

(8) Mattisson, T.; Zafar, Q.; Lyngfelt, A.; Johansson, M. Chemical Looping Combustion as a new CO_2 management Technology. Presented at the 1st Regional Symposium on Carbon Management, Dhahran, Saudi Arabia, May 22−23, 2006.

(9) Zafar, Q.; Mattisson, T.; Gevert, B. *Energy Fuels* **2006**, *20*, 34−44.

(10) Villa, R.; Cristiani, C.; Groppi, G.; Lietti, L.; Forzatti, P.; Cornaro, U.; Rossini, S. *J. Mol. Catal., A: Chem.* **2003**, *204−205*, 637−646.

(11) Mattisson, T.; Johansson, M.; Lyngfelt, A. *Fuel* **2006**, *85*, 736−747.

(12) Johansson, E.; Mattisson, T.; Lyngfelt, A, Thunman, H. *Fuel* **2006**, *85*, 1428−1438.

(13) Ryden, M.; Lyngfelt, A.; Mattisson, T. *Fuel* **2006**, *85*, 1631−1641.

(14) Ishida, M.; Jin, H.; Okamoto, T. *Energy Fuels* **1996**, *10*, 958−963.

(15) Ryu, Ho-J.; Bae, D-H.; Han, K-H.; Lee, S-Y.; Jin, G-T.; Choi, J-H. *Korean J. Chem. Eng.* **2001**, *18* (6), 831−837.

(16) Garcia-Labiano, F.; de Diego, L. F.; Adanez, J.; Abad, A.; Gayan, P. *Ind. Eng. Chem. Res.* **2004**, *43*, 8168−8177.

(17) Garcia-Labiano, F.; Adanez, J.; de Diego, L. F.; Gayan, P.; Abad, A. *Energy Fuels* **2006**, *20*, 26−33.

(18) Abad, A.; Adanez, J.; Garcia-Labiano, F.; de Diego, L. F.; Gayan, P.; Celaya, J. *Chem. Eng. Sci.* **2007**, *62*, 533−549.

(19) Son, S. R.; Kim, S. D. *Ind. Eng. Chem. Res.* **2006**, *45*, 2689−2696.

(20) Readman, J. E.; Olafsen, A.; Smith, J. B.; Blom, R. *Energy Fuels* **2006**, *20*, 1382−1387.

**Table 1. Properties of the NiO/MgAl₂O₄ Oxygen Carrier Particles**

theoretical NiO content (wt %)	60
active NiO content (wt %)	50
particle size (mm)	0.125−0.180
porosity	0.36
specific surface area BET (m^2/g)	3.0
apparent density (kg/m^3)	3200
molar density of NiO/MgAl₂O₄ (mol/m^3)	33 290
molar density of Ni/MgAl₂O (mol/m^3)	47 712
grain radius of NiO/MgAl₂O (m)	0.2×10^{-6}
grain radius of Ni/MgAl₂O (m)	0.19×10^{-6}

for 6 h at 1400 °C to increase the mechanical strength. During sintering of the oxygen carrier, some of the NiO reacted with the support material and formed irreversible phases, likely spinels.[9] Oxygen carrier particles were sieved to get a size range between 125 and 180 μm. The preparation method has been discussed in detail by Mattisson et al.[11] The main physical properties of the NiO/MgAl₂O₄ oxygen carrier are given in Table 1

2.2. Reactivity Investigation. The experiments were performed in a high-resolution thermogravimetric analyzer (TGA 2950, TA Instruments). The reactor was an evolved gas analysis (EGA) furnace which consisted of a quartz tube (15 mm i.d.), and the sample holder was a platinum pan (9 mm i.d.). The reacting gas enters from one side of the quartz tube, reacts with the sample, and leaves the tube from other side, as shown in Figure 2. The lower part was filled with inert quartz particles to reduce the volume of the reactor tube.

A 20 mg sample of the oxygen carrier NiO/MgAl₂O₄ was heated in the platinum pan to the desired reaction temperature (800−1000 °C) in a nitrogen atmosphere. The particles were well-spread in the platinum pan forming a single layer, in order to avoid the interparticle mass transfer resistance. The sample was exposed in a cyclic manner to a reducing gas of 5−20% CH₄ and 20% H₂O balanced with N₂ for the reduction period and to an oxidizing gas of 3−15% O₂ balanced with N₂ for the oxidation period. The CH₄ and O₂ concentration used in the experiments are in the range of the average gas concentration, which the particles may be exposed to in the fuel and air reactors. The steam was added during the reduction period to avoid any carbon formation on the particles but also to better simulate the environment to which the particles are exposed to in the fuel reactor. The reduction period was 50−140 s, and the oxidation period was 70−150 s long, depending on the reaction temperature and reacting gas concentration used in the experiment. N₂ was introduced for 200 s after each reducing and oxidizing period to avoid mixing between methane and oxygen.

The flow of the gas into the reactor was controlled by electronic mass flow regulators and was 300 mL/min (normalized to 1 bar and 0 °C) for all the periods and cycles. A 10% portion of the total gas flow, i.e., 30 mL/min purge N₂, was always introduced from the head of the TGA to keep the balance parts free from any corrosive gas. Some tests were performed with different gas flows,
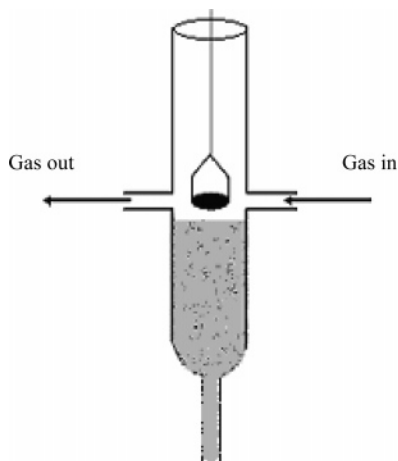
Figure 2. TGA furnace used for reactivity experiments.

and no effect on reaction rate was observed; thus, it was concluded that mass transfer resistance is not rate limiting in these experiments. However, in the initial part of the reaction, the reaction rate increased for 3−5 s, depending on the temperature and the gas concentration used in the experiment. This is likely due to some small back-mixing in the system, and thus, there is a short time when the methane concentration is lower than the desired concentration. In the experiments, the gas flow was relatively high and the reactor volume was small; thus, calculations showed that the gas residence time in the reactor should be less than 0.5 s. Due to this short delay time, the measured reactivity data for the first few seconds was not used in the calculations, but instead, the rate was here obtained from extrapolation of data obtained when there was no back-mixing. At least four cycles of reduction and oxidation were performed for each experiment. The reactivity during the first cycle was generally somewhat slower in comparison to the succeeding ones, and here, the fourth cycle is used as the reference cycle.

The degree of conversion for reduction and oxidation was calculated as

$$X_{red} = 1 - \frac{(m - m_{red})}{(m_{ox} - m_{red})} \tag{3}$$

$$X_{ox} = \frac{(m - m_{red})}{(m_{ox} - m_{red})} \tag{4}$$

The difference between m_{ox} and m_{red} in eqs 3 and 4 is the amount of active oxygen in the carrier, i.e., the maximum amount of oxygen that can be transferred through reaction with methane. The difference between m_{ox} and m_{red} is calculated on the basis of the transformation between NiO and Ni. Although the oxygen carrier was prepared with 60% NiO, by reducing the sample in an H₂ atmosphere, the actual oxygen capacity was found to be somewhat less, likely due to reactions between inert and active metal oxide, and as is shown in Table 1; the active NiO content here is 50%.

3. Results

3.1 Reduction Reaction. In the fuel reactor, the oxygen carrier is exposed to different fuel gas concentrations and environments at different locations. At the bottom of the fluidized bed, oxygen carrier will be in contact with pure fuel while the gas phase will mostly consist of CO₂ and H₂O at the top of the bed. Some experiments were done by adding 5% CO₂ with fuel gas to see the effect of product CO₂ on the reduction reaction with oxygen carrier; however, no major change in reaction rate was observed.

The reaction of methane with NiO is an example of noncatalytic solid−gas reaction, and several resistances can affect the reaction rate. The reaction could be controlled by external mass transfer, gas diffusion into the porous particle, diffusion in the solid product layer, and the chemical reaction. Mass transfer resistance was reduced as much as possible by working with high gas flows and small sample masses in the TGA experiments. The effect of particle size was investigated with particles in the size range 90−250 μm, and no effect on the reaction rate was observed. This suggests that internal diffusion resistance is not limiting the rate of reaction. The oxygen carrier particles are porous and porosity increases as NiO is reduced to Ni due to the difference in molar density of NiO and Ni; see Table 1. Garcia-Labiano et al. showed that for the experimental conditions (porosity, type and content of MeO, particle size, and reaction rate) similar to those used in this work, internal diffusion resistance is not important, and the reaction

takes place inside the whole particle at the same time.[21] Also, temperature changes inside the particle due to reactions were not important and the particles could be considered isothermal. Chemical reaction seems to be the only resistance which is controlling the reduction reaction rate of these types of oxygen carriers with methane.

During the preparation of the freeze-granulated particle, small primary particles of NiO and $MgAl_2O_4$ of less than 10 μm in size are physically mixed and prepared into a slurry which can easily be atomized into drops of larger size. Thus, the particles are composed of relatively large individual grains/primary particles. This was also confirmed by environmental scanning electron microscope (ESEM) images of the surface of the particles. Thus, for kinetic determination, it was assumed that the particles are composed of spherical grains, which react with the same reaction rate throughout the particle following the shrinking-core model. The kinetics equation for the shrinking-core model for a spherical grain with chemical reaction control is[22]

$$\frac{t_{ch}}{\tau_{ch}} = 1 - (1 - X)^{1/3} \qquad (5)$$

where τ_{ch} is the time for complete conversion of the particle and calculated from

$$\tau_{ch} = \frac{\rho_m r_g}{bkC^n} \qquad (6)$$

which can be rearranged to

$$\ln\left[\frac{\rho_m r_g}{b\tau_{ch}}\right] = \ln(k) + n \ln C_{CH_4} \qquad (7)$$

3.1.1. Effect of CH₄ Concentration. To see the effect of the methane concentration on the reduction of $NiO/MgAl_2O_4$ carrier, experiments were performed with 5, 10, 15, and 20% CH_4. Fuel gas was saturated with water vapors (20%) in all the experiments to avoid carbon formation on the particles. Figure 3 shows the solid conversion as a function of time for $NiO/MgAl_2O_4$ oxygen carrier with different CH_4 concentrations at 950 °C for the fourth reduction period. Also included in the figure are the results of the model calculations, i.e., eq 5, using the kinetic parameters obtained in this work; see below. The reaction rate is very fast initially for all experiments, and the reaction rate increased with increasing CH_4 concentration. For all concentrations, less than 20 s is needed to obtain $\Delta X = 0.6$.

3.1.2. Effect of Temperature on the Reduction Reaction. The effect of temperature on the reduction reaction was also investigated. Several experiments were done with different CH_4 concentrations, i.e., 5, 10, 15, and 20%, at different temperatures from 800 to 1000 °C. Figure 4 shows the conversion as a function of time obtained with a 10% CH_4 concentration at different temperatures. Clearly, the reaction rate is a function of temperature. The change in conversion was very low at lower temperatures, i.e., conversion was only $\Delta X = 0.2$ and 0.4 at 800 and 850 °C, respectively. However, at these temperatures, the reactions were relatively fast in the beginning of reduction but decreased rapidly and continue at a very slow rate. It is likely that at lower temperatures the reaction is controlled by
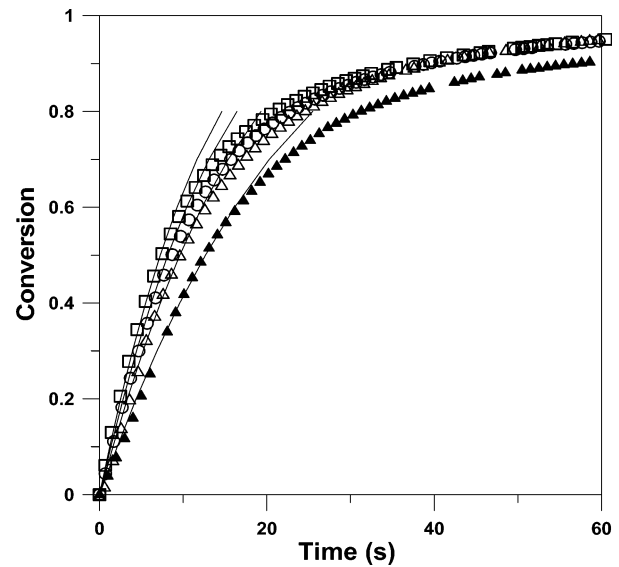
(21) Garcia-Labiano, F.; de Diego, L. F.; Adanez, J.; Abad, A.; Gayan, P. *Chem. Eng. Sci.* **2005**, *60*, 851−862.

(22) Levenspiel, O. *Chemical Reaction Engineering*, 3rd ed.; John Wiley & Sons: New York, 1999.

Figure 3. Conversion as a function of time for different CH_4 concentrations for the experiments conducted at 950 °C. CH_4 concentrations are 5% (▲), 10% (△), 15% (○), and 20% (□). The continuous lines are results predicted by the model using kinetic parameters obtained in this work.
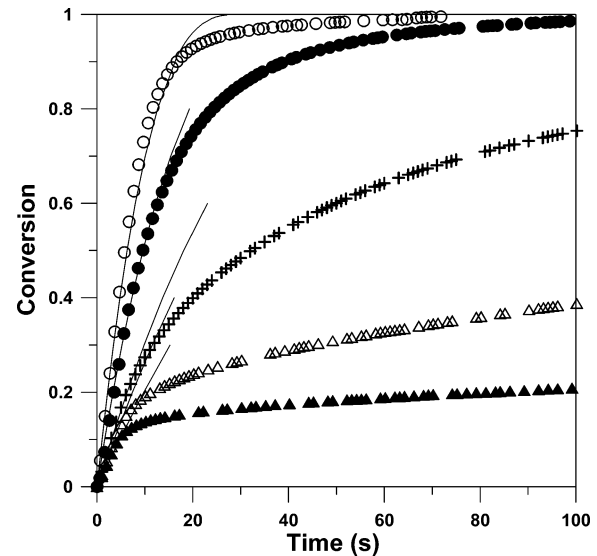

Figure 4. Effect of temperature on the reduction reaction of $NiO/MgAl_2O_4$ with CH_4 (10%) at 800 (▲), 850 (△), 900 (+), 950 (●), and 1000 °C (○). The continuous lines are results predicted by the model using kinetic parameters obtained in this work.

two kinds of different resistance; at low solid conversion, the reaction rate is likely controlled by chemical reaction, and at higher solid conversion (from 0.1 to 1 depending on the temperature), the reaction rate could be controlled by the diffusion in the solid product layer. Because of the slow reduction reaction at lower temperatures, the investigated particles should likely be used at temperatures of 900 °C and above. Here, the reaction is controlled by chemical reaction for a substantial part of the conversion interval; see Figure 4.

3.1.3. Kinetic Parameters for the Reduction Reaction. Figure 5 shows a plot of $\ln(\rho_m r_g/b\tau)$ as a function of $\ln(C_{CH_4})$ for the experiments conducted at different temperatures. The slope of the plot was about 0.4 with all temperatures, which is the order of reaction n with respect to CH_4. Also, the values of k at different temperatures were obtained from the y-intercept in the figure.
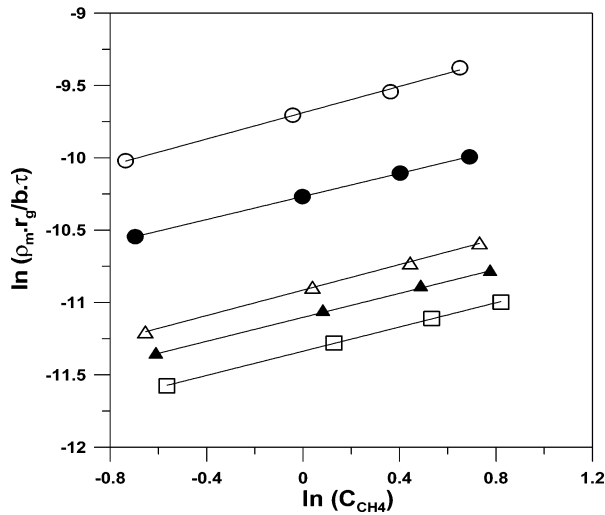
Figure 5. Plot of $\ln(\rho_m r_g/b\tau)$ as a function of $\ln(C_{CH_4})$ to obtain the order of reaction for reduction and the value of k at different temperatures: 800 (□), 850 (▲), 900 (△) 950 (●), and 1000 °C (○).
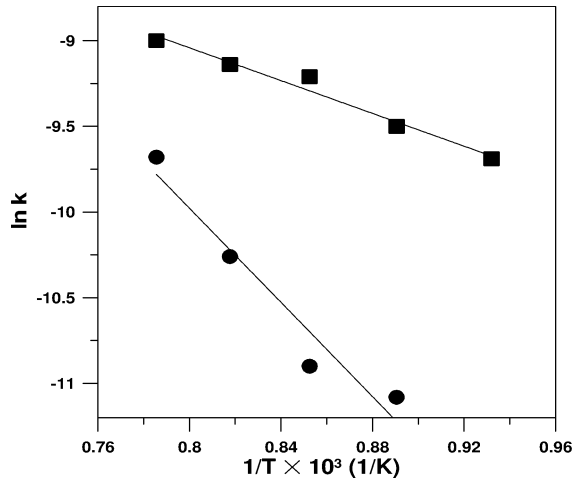

Figure 6. Arrhenius plot of the reduction and oxidation reactions with NiO/MgAl₂O₄ oxygen carrier: CH_4 (●), O_2 (■).

Table 2. Kinetic Parameters for the Reduction and Oxidation Reactions of the NiO/MgAl₂O₄ Oxygen Carrier

	CH_4	O_2
E (kJ/mol)	114	40
k_o ((mol^{1-n} m^{3n-2})/s)	2.75	5.43×10^{-3}
n	0.4	1.0

Figure 6 shows the plot used to obtain the values of the kinetic parameters assuming an Arrhenius dependence of the kinetic constant with the temperature,

$$k = k_o e^{(-E/RT)} \tag{8}$$

Results from the investigation at 800 °C have not been included in the plot due to the low conversion at this temperature. The frequency factor, k_o, and activation energy, E, obtained are shown in Table 2. The value of activation energy for the reduction reaction was found to be 114 kJ/mol, and the frequency factor, k_o, was 2.75 mol$^{0.6}$/(m$^{0.8}$ s). The value of the activation energy found here is higher in comparison with the values found by the other authors for NiO using YSZ, bentonite, and alumina as inert materials.[14,15,18] This is possibly due to the addition of MgO in the oxygen carrier, where a NiO−MgO solid solution may form, in which Ni^{2+} ions are stabilized against reduction and sintering by an MgO-type matrix as shown
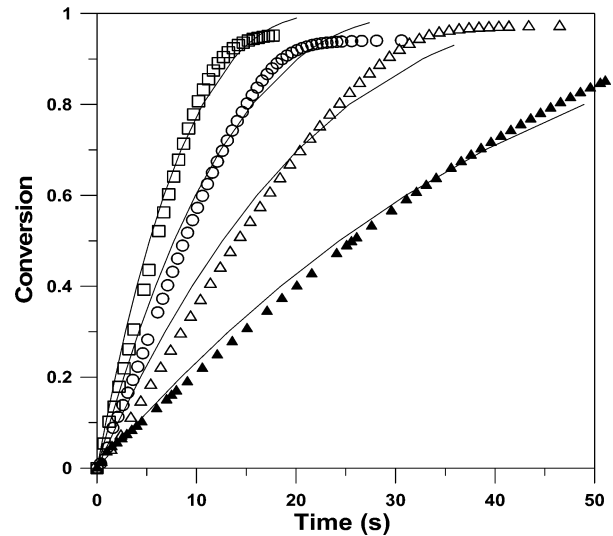

Figure 7. Conversion as a function of time for different O_2 concentrations for the experiments conducted at 1000 °C. O_2 concentrations are 3 (▲), 6 (△), 10 (○), and 15% (□). The continuous lines are results predicted by the model using kinetic parameters obtained in this work.

by Villa et al.[10] These authors analyzed the reactivity of the oxygen carrier by temperature-programmed reduction (TPR), and it could be speculated that the presence of Mg in the particles increases the reduction temperature peak in the TPR analysis, thus increasing the activation energy of the reaction.

The kinetic constant, k, obtained from eq 8 using the frequency factor and activation energy from Table 2, and the order of reaction, n, were used in the shrinking-core model, eq 6. The model results are shown together with the experimental data in Figures 3 and 4. The experimental results are represented by symbols, and the model predictions are represented by continuous lines. It can be seen in Figures 3 and 4 that experimental results obtained at temperatures of practical interest (950 and 1000 °C) fit with the prediction model until almost 70% conversion of the oxygen carrier during reduction. It is unlikely that NiO/MgAl₂O₄ will be reduced to such a high degree of conversion in the fuel reactor of a real chemical-looping combustor, since a high degree of conversion difference between the air and fuel reactors would mean large temperature drops in the fuel reactor.

3.2. Oxidation Reaction. The reduced oxygen carrier from the fuel reactor will be transferred to the air reactor of a CLC system for regeneration. In the air reactor, NiO/MgAl₂O₄ oxygen carrier in reduced state will be exposed to different oxygen concentrations varying from 21% O_2 at the inlet of the reactor and perhaps 4% O_2 at the outlet if a 20% of excess air is used in the reaction. Several experiments were conducted with different oxygen concentrations between 3 and 15% at different temperatures 800−1000 °C to determine the kinetics of the oxidation reaction.

3.2.1. Effect of O_2 Concentration. Figure 7 shows the conversion as a function of time obtained at 1000 °C with different oxygen concentrations for the fourth oxidation period. Also shown are the model calculations using kinetic data obtained below. Clearly, also the oxidation reaction is very fast and the rate of reaction is a function of the oxygen concentration with the higher rates for the experiments corresponding to the higher oxygen concentration.

3.2.2. Effect of Temperature on the Oxidation Reaction. The effect of temperature on the oxidation reaction was investigated by performing several experiments at different temperatures
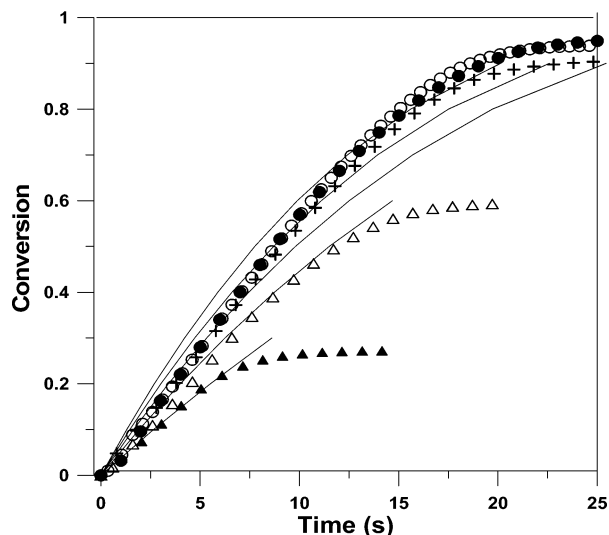
Figure 8. Effect of temperature on the oxidation reaction of NiO/MgAl$_2$O$_4$ with O$_2$ (10%) at 800 (▲), 850 (△), 900 (+), 950 (●), and 1000 °C (○). The continuous lines are results predicted by the model using kinetic parameters obtained in this work.

Figure 9. Plot of ln($\rho_m r_g/b\tau$) as a function of ln(C_{O_2}) to obtain the order of reaction for oxidation and the value k at different temperatures: 850 (▲), 900 (△) 950 (●), and 1000 °C (○).

between 800 and 1000 °C with different O$_2$ concentrations of 3, 6, 10, and 15% to increase the validity of the data.

Figure 8 shows the conversion as a function of time obtained at different temperatures with 10% O$_2$ concentrations. It was observed that the oxidation rate was a function of temperature; although for higher temperatures, i.e., 900, 950, and 1000 °C, there is only a little difference in the reaction rate. The low degree of final conversion at 800 and 850 °C is due to the low conversion reached during the reduction period. But in all cases, the sample was oxidized back to a fully oxidized sample.

3.2.3. Kinetic Parameters for the Oxidation Reaction. The shrinking-core model for spherical grains was also used to model the oxidation reaction, i.e., eq 5. The kinetic model was developed using chemical reaction as the only resistance controlling the reaction. To determine the order of reaction, several experiments were conducted at different temperatures with different O$_2$ concentrations. The reaction order, *n*, of the oxidation reaction was obtained by the slope of the plot of ln-($\rho_m r_g/b\tau$) vs ln(C_{O_2}) and was about 1; see Figure 9. The results obtained at 800 °C have not been included in this figure due to the much lower conversion obtained in the previous reduction step at this temperature.

Figure 6 shows the Arrhenius plot obtained from the oxidation reaction data. The energy of activation for oxidation reaction obtained from the Arrhenius plot was about 40 kJ/mol, and the pre-exponential factor k_o found was 5.43×10^{-3} m/s.

The results obtained with the shrinking-core model fit reasonably well with the experimental results—see Figures 7 and 8—which confirms that chemical reaction controlled the global reaction rate.

4. Design of a CLC System

The main parameters for the design of a CLC system are (i) the amount of oxygen carrier in both reactors must be enough in order to convert all the incoming reacting gases and (ii) the recirculation rate between the air and fuel reactors must be high enough to transport oxygen necessary for the fuel combustion and supply enough heat to maintain the high temperature in the fuel reactor, where the reaction of CH$_4$ with the Ni-based oxygen carrier is endothermic.
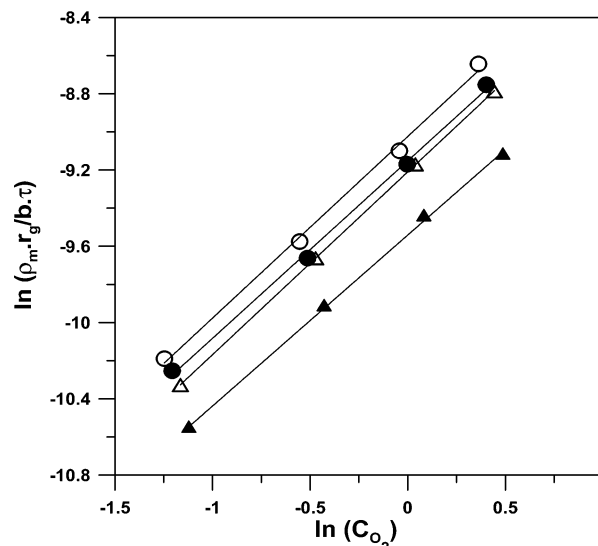
4.1. Mass and Heat Balance. In CLC, oxygen is transported from air reactor to the fuel reactor by means of oxygen carrier. It is expected that a small amount of oxygen carrier will be elutriated from the reactor system due to attrition/fragmentation during the operation. Thus, a makeup flow of oxygen carrier will be necessary in order to maintain the mass balance in the reactor system. However, it is likely that this makeup is too low to have any effect on mass and heat balance and was not considered in the calculations. Also, when ash-free gaseous fuel is used, it is possible that elutriated material can be used as raw material in the production process for the oxygen carrier particles.

The reaction of NiO with methane is endothermic, which results in a temperature drop in the fuel reactor. In order to maintain a high reduction rate of oxygen carrier particles with methane, a large temperature drop in the fuel reactor must be avoided. The temperature drop in the fuel reactor depends on the circulation rate of oxygen carrier, which is connected to the conversion difference of oxygen carrier between in the air and fuel reactors. A heat balance was made over the CLC reactor system for NiO/MgAl$_2$O$_4$ oxygen carrier. Here, it was assumed that the fuel gas was preheated to 400 °C before it was introduced to the fuel reactor and that 20% excess air was used. It was found that in order to achieve a working temperature of 1000 °C in the air reactor and 950 °C in the fuel reactor, the conversion difference, ΔX, should be 0.18 for NiO/MgAl$_2$O$_4$ with 50% active NiO content.

4.2. Recirculation Rate. The recirculation rate depends on the oxygen carrier and fuel used, as well as on the active metal content and the conversion variation obtained in the fuel and air reactors. The method of calculation for the recirculation rate is based on the work of Abad et al.[18] For 1 MW$_f$ and assuming full conversion of fuel gas, the recirculation rate can be calculated from the following equation,

$$\dot{m}_{OC} = \frac{\dot{m}_c}{\Delta X_{S,FR}} \tag{9}$$

where $\dot{m}_c$ is the characteristics circulation rate and is defined by the oxygen carrier transport capacity and fuel,

$$\dot{m}_c = \frac{2dMo}{R_{o,OC}\Delta H_c^{\circ}} \tag{10}$$

A value of 0.74 kg/(s MW) for $\dot{m}_c$ was obtained using NiO/MgAl₂O₄ (50% active NiO content) as an oxygen carrier and methane as fuel. As discussed earlier, in the case of NiO oxygen carrier, the recirculation rate is limited by the heat balance, due to the endothermic reaction in the fuel reactor. The recirculation rate of oxygen carrier per MW$_f$ of CH₄ was 4.14 kg/s, when ΔX was 0.18. To achieve a reasonable recirculation flux of iron oxide particles between the air and fuel reactors, Lyngfelt et al. proposed, a high velocity riser, similar to the actual configuration of a circulating fluidized bed boiler (CFB). The authors found that a recirculation rate of 50 kg/(m² s) was needed to transport sufficient oxygen, and this was deemed feasible in the proposed system.[3] The recirculation rate in a CFB depends on the operational conditions and riser configuration. The value of the riser area in a CLC process for the combustion of methane was suggested to be in the range 0.18−0.35 m²/MW$_f$.[18] Taking a value of 0.2 m²/MW$_f$ as an average of the cross-sectional area of a riser, S, the solid flow can be calculated as

$$G_s = \frac{\dot{m}_{OC}}{S} \tag{11}$$

The value of G_s found was 20.7 kg/(m² s) for the NiO/MgAl₂O₄ oxygen carrier used in this work which should be within the normal operational range for CFB systems.

4.3. Solid Inventory. The NiO/MgAl₂O₄ oxygen carrier has been investigated in a 300 W CLC reactor system in the work of Johansson et al.[12] Complete conversion of methane was obtained using a solid inventory in the range 600−2200 kg/MW$_f$. However, from this result, it can be deduced that the amount of oxygen carrier material in the CLC system should be less while still maintaining high gas yield. This would be preferable in order to reduce the reactor size, which will result in a lower investment cost in addition to less production cost for oxygen carrier particles. A lower bed mass will also consume less power from the fans that supply reacting gases to the air and fuel reactors. Thus, it is desirable to optimize the amount of bed material in a CLC system. The amount of bed material in a CLC system is directly related to the reactivity of the oxygen carrier with the fuel gas and air, as well as the oxygen transport capacity. NiO has a rather high transport capacity in comparison with Fe₂O₃ and Mn₃O₄, which are other common oxygen carrier materials.

The calculation method for the solid inventory is based on the method proposed by Abad et al.[18] For the complete conversion of gas, the bed mass in each reactor per MW of fuel can be calculated as

$$m_{OC,FR} = \dot{m}_c \frac{\tau_r}{\phi_{FR}} \tag{12a}$$

$$m_{OC,AR} = \dot{m}_c \frac{\tau_o}{\phi_{AR}} \tag{12b}$$

where the parameters ϕ_{FR} and ϕ_{AR} are the characteristics reactivities in the fuel reactor and air reactor, respectively, and are defined as

$$\phi_{FR} = \left[\tau_r \overline{\frac{dX_S}{dt}}\right]_{FR} \tag{13a}$$

$$\phi_{AR} = \left[\tau_o \overline{\frac{dX_S}{dt}}\right]_{AR} \tag{13b}$$

The parameters τ_r and τ_o in eqs 12 and 13 are the times needed for the complete conversion of particles in the fuel and air reactors, respectively, obtained at an average gas concentration and $\overline{dX_S/dt}$ is the average solid reactivity in the air and fuel reactors. Assuming gas plug flow in the reactors and no resistance to the gas exchange between the bubble and emulsion phases in the fluidized bed, the average reacting gas concentration in the fuel and air reactors can be obtained by the equation,

$$\bar{C}_n = \frac{\Delta X_g C_0^{\,n}}{\int_{X_{g,in}}^{X_{g,out}} \left[\frac{1 + \epsilon_g X_g}{1 - X_g}\right]^n dX_g} \tag{14}$$

The parameter ϵ_g in eq 14 represents the gas volume variation as a result of reaction and can be calculated as

$$\epsilon_g = \frac{V_{g,X_g=1} - V_{g,X_g=0}}{V_{g,X_g=0}} \tag{15}$$

When CH₄ is used as the fuel gas in CLC, for each mole of reacting gas, 3 mol of product gas are obtained. The value of ϵ_g is 2 for the reduction reaction, using CH₄ as the fuel gas, while it is −0.21 for the oxidation reaction. Considering 100% CH₄ at the inlet of the fuel reactor and a final gas conversion of 0.999, the average CH₄ concentration obtained in the fuel reactor was 13.2%. The average concentration of oxygen in the air reactor was 11%, using 20% excess air for combustion. The values of τ_r and τ_o obtained in this work were 42 and 34 s, respectively, considering the temperature in the fuel reactor as 950 °C and that in the air reactor as 1000 °C.

With the assumption of perfect mixing of solid particles in the fuel and air reactors, the characteristic reactivity, ϕ_j, can be expressed as a function of solid conversion at the inlet of each reactor and the conversion variation in a reactor. For a spherical grain ϕ_j can be calculated as[18]

$$\phi_j = 3\left[1 - X_{o,inj}^{\,2/3} \exp\left(-\frac{(1 - X_{o,inj}^{\,1/3})}{\Delta X_S}\phi_j\right)\right] - 6\frac{\Delta X_S}{\phi_j}\left[1 - X_{o,inj}^{\,1/3} \exp\left(-\frac{(1 - X_{o,inj}^{\,1/3})}{\Delta X_S}\phi_j\right)\right] + 6\frac{\Delta X_S^{\,2}}{\phi_j^{\,2}}\left[1 - \exp\left(-\frac{(1 - X_{o,inj}^{\,1/3})}{\Delta X_S}\phi_j\right)\right] \tag{16}$$

The value of characteristic reactivity is limited between 0 and 3 for the spherical grain using the shrinking-core model.

Total solid inventory in a CLC system is obtained by summation of the bed masses in the fuel and air reactors

$$m_{total} = m_{OC,FR} + m_{OC,AR} \tag{17}$$

The parameter ϕ_j varies with the solid conversion at the inlet of the fuel or air reactor, varying the solid inventory. The minimum solid inventory in a CLC system of interconnected fluidized beds is defined by the solid−gas reactivity and depends on τ_r and τ_o.

Abad et al. have shown the curves of τ_r/τ_o and τ_o/τ_r to obtain the minimum solid inventory for CLC.[18] For $\Delta X_S = 0.18$ and with $\tau_r = 42$ s for the reduction reaction and $\tau_o = 34$ s for the
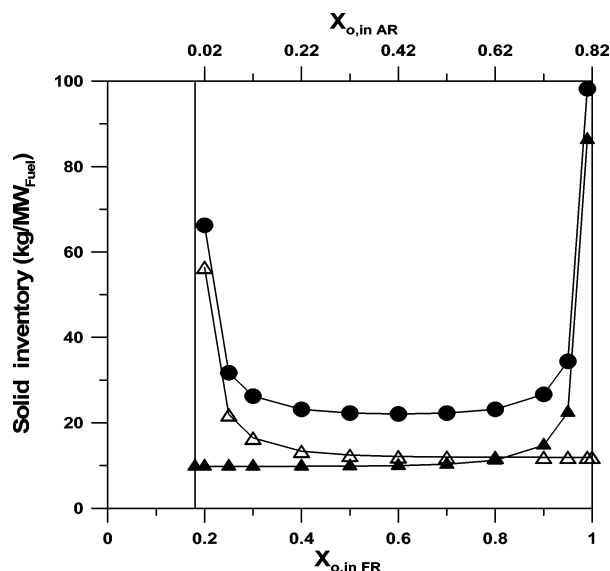
Figure 10. Solid inventory as a function of solid conversion at the inlet of the fuel reactor ($X_{o,inFR}$) and the air reactor ($X_{o,inAR}$), m_{FR} ($\triangle$), m_{AR} ($\blacktriangle$), and m_{total} ($\bullet$).

oxidation reaction, the minimum solid inventory in the fuel reactor is reached at a point ($\Delta X_S = 0.18$, $\tau_r/\tau_o = 1.2$) which gives values for $\phi_{FR} = 2.58$ and $X_{o,inFR} = 0.6$. For the air reactor, at point ($\Delta X_S = 0.18$, $\tau_o/\tau_r = 0.8$), the values of $\phi_{AR} = 2.57$ and $X_{o,inAR} = 0.42$ were obtained. Figure 10 shows the total solid inventory needed in the reactors system. It can be seen that total solid inventory is dependent on the solid conversion at the inlet of the fuel and air reactors. The minimum solid inventory needed in this work obtained was 22 kg/MW$_f$. The solid inventory increases as the solid conversion approaches the value of $X_{o,inFR} = 0.18$ or complete conversion in the air reactor.

5. Discussion

The kinetics of a promising oxygen carrier $NiO/MgAl_2O_4$ has been investigated in TGA using CH_4 as a reducing gas and O_2 as an oxidizing gas. The oxygen carrier was prepared by freeze-granulation and has earlier been investigated in both continuous and batch-fluidized beds with highly promising results. However, the detailed kinetics for the particles has not been investigated earlier, and this was done in the present work. It was found that both the reduction and oxidation rates were dependent on the concentration of reacting gases and the reaction temperature.

The reaction orders, n, found for $NiO/MgAl_2O_4$ with CH_4 and O_2 were 0.4 and 1, respectively. There is no data available in the literature concerning the reaction order of this type of oxygen carrier with methane and oxygen. Abad et al. investigated a carrier based on NiO with Al_2O_3 and found reaction orders of 0.8 and 0.2 for CH_4 and O_2, respectively.[18] Readman et al. also investigated NiO on $NiAl_2O_4$ and found reaction order of 0.74 and 1 for CH_4 and O_2 respectively[20]. The two types of particles are clearly different, and the difference in the values of reaction order may be due to Mg addition in the oxygen carrier used in this work.

The activation energies found for reduction and oxidation reactions were 114 and 40 kJ/mol, respectively. A number of publications have calculated the activation energy for the reduction and oxidation reactions for Ni-based oxygen carriers.[14,15,18,19] The activation energy obtained in this work is rather high in comparison to those found for previously investigated Ni-based oxygen carriers. As discussed earlier, possibly, addition

of Mg in the oxygen carrier increases the activation energy both for the reduction and oxidation reactions.

The solid inventory needed in a CLC system is inversely proportional to the reactivity of the metal oxide with fuel and oxygen. $NiO/MgAl_2O_4$ showed a very high reaction rate during both reduction and oxidation at high temperatures. Thus, a lesser amount of this oxygen carrier will be needed in the CLC reactor system. For $NiO/MgAl_2O_4$ oxygen carrier, the minimum solid inventory with a solid conversion of $\Delta X_S = 0.18$, is 22 kg/MW$_f$. This amount can be compared with the amount of Ni-based oxygen carriers calculated by other authors. Mattisson et al. investigated NiO/Al_2O_3 prepared by impregnation in a TGA and found that the total solid inventory needed for CLC is 620 kg/MW.[23] Zafar et al. investigated $NiO/MgAl_2O_4$ prepared by impregnation and concluded that the amount of oxygen carrier needed in the fuel and air reactors varies between 125 and 175 kg/MW depending on the mass-based conversion difference, $\Delta\omega$, obtained in the reactor system .[9] However, these authors assumed first-order reaction with average CH_4 and O_2 concentrations of 10 and 5% in the fuel and air reactors, respectively. Also, the active NiO content in these particles was below 30%. Cho et al. investigated freeze-granulated NiO on alumina support in a laboratory fluidized bed reactor and found that $57-162$ kg/MW oxygen carrier is needed in the fuel reactor depending on the mass-based solid conversion achieved during reduction.[24] Readman et al. have presented reactivity data for $NiO/NiAl_2O_4$ oxygen carrier containing a 60 wt % active metal content. The solid inventory needed in the fuel and air reactors of a CLC system, based on the reactivity data given, is 315 kg/MW$_{fuel}$.[20] Abad et al. found an inventory of 45 kg/MW$_f$ of freeze-granulated NiO on alumina support with an active MeO content of 40 wt %.[18] The above discussion shows that the oxygen carrier used in this work needs a lesser amount of bed material per MW of fuel and is superior to the oxygen carriers investigated by the other authors using methane as fuel. All authors assumed that mass transfer resistance was negligible between the bubble and emulsion phase. When the mass transfer in the fluidized bed is important, the solids inventories should be higher than those given.

6. Conclusions

The detailed reactivity of a highly promising oxygen carrier for CLC was determined using methane and oxygen. The carrier was composed of 60 wt % NiO with 40 wt % $MgAl_2O_4$. Some of the NiO reacted with the support material, reducing the active content to approximately 50%. The reactivity was investigated in a TGA at $800-1000$ °C using $5-20\%$ CH_4 as a fuel gas for reduction and $3-15\%$ O_2 as an oxidizing gas for oxidation. The oxygen carrier showed very high reactivity during reduction and oxidation. The reaction rate was a function of the reacting gas concentration and temperature both for the reduction and oxidation reactions. However, conversion of particles for the reduction reaction was very low at lower temperatures, i.e., 800 and 850 °C, suggesting that it may not be feasible to use this oxygen carrier at lower temperatures in a CLC system. The shrinking-core model for the spherical grain geometry of a reacting particle with chemical reaction control was used to determine the kinetics of reduction and oxidation. The value of the reaction order for the reduction reaction was 0.4, while it was found to be 1 for the oxidation reaction. The activation

(23) Mattisson, T.; Järdnäs, A.; Lyngfelt, A. *Energy Fuels* **2003**, *17*, 643−651.

(24) Cho, P.; Mattisson, T.; Lyngfelt, A. *Fuel* **2004**, *83*, 1215−1225.

energy for the reduction and oxidation reactions found was 114 and 40 kJ/mol, respectively. The values of activation energy are higher than those described in the literature for Ni-based oxygen carrier. This may be due to the addition of MgO in the oxygen carrier particles. The reactivity data of NiO/MgAl₂O₄ was used to estimate the solid inventory needed in the CLC system. It was found that the total solid inventory varies with the solid conversion at the inlet of the fuel and air reactors. The minimum solid inventory found was 22 kg/MW$_f$. In order to operate the fuel reactor at 950 °C and the air reactor at 1000 °C, the solid conversion difference between the two reactors should not be more than 0.18, with a recirculation rate of 4.15 kg/(s MW$_f$).

Nomenclature

b_i = stoichiometric factor for the reaction i, mol solid reactant
C_i = gas concentration of species i, mol/m
d = stoichiometric factor in the fuel combustion reaction with oxygen, mol O_2/mol fuel
E = activation energy, kJ/mol
G_s = specific solids circulation rate, kg /(m² s)
k = chemical reaction rate constant, $(mol^{1-n} \, m^{3n-2})/s$
k_0 = pre-exponential factor of the chemical reaction rate constant, $(mol^{1-n} \, m^{3n-2})/s$
$m_{OC,FR}$ = solid inventory, in the fuel reactor, kg OC/MW$_f$
$m_{OC,AR}$ = solid inventory, in the air reactor, kg OC/MW$_f$
m_{total} = total solid inventory, as fully oxidized oxygen carrier, kg OC/MW$_f$

$\dot{m}_c$ = characteristic circulation rate, kg OC/(s MW$_f$)
$\dot{m}_{OC}$ = circulation rate of fully oxidized oxygen carrier, kg OC/(s MW$_f$)
M_O = molecular weight of oxygen, 16 g/mol
m = actual mass of the oxygen carrier, g
m_{red} = mass of the sample in reduced form, g
m_{ox} = mass of the sample when it is fully oxidized, g
n = reaction order
$R_{o,OC}$ = oxygen transport capacity of the oxygen carrier
r_g = grain radius, m
S = cross-sectional area of the riser per MW$_f$, m²/MW$_f$
t = time, s
$V_{g,X_g=0}$ = volume of the gas mixture at $X_g = 0$, m³
$V_{g,X_g=1}$ = volume of the gas mixture at $X_g=1$, m³
X_{red} = the degree of conversion during reduction of oxygen carrier
X_{ox} = the degree of conversion during oxidation of oxygen carrier
X_g = gas conversion
$X_{g,in}$ = gas conversion at the reactor inlet
$X_{g,out}$ = gas conversion at the reactor outlet
X_s = solid conversion
$X_{o,inj}$ = average solid conversion at the inlet of the reactor j

Greek Letters

ΔH_c° = standard heat of combustion of the gas fuel, kJ/mol
ΔX_g = variation of the gas conversion
ΔX_s = variation of the solid conversion between the two reactors
ϵ_g = coefficient of expansion of the gas mixture
ϕ_j = characteristic reactivity in the reactor j
ρ_m = molar density of the reacting material, mol/m³
τ_{ch} = time required for complete conversion of the particles, s
τ_r = time needed for the complete conversion of particles in the fuel reactor, s
τ_o = time needed for the complete conversion of particles in the air reactor, s